Biogeochemistry **62:** 59–86, 2003.

Spatial variation in pyritization of trace metals in salt-marsh soils

XOSE L. OTERO* and FELIPE MACIAS
*Departamento de Edafoloxía e Química Agrícola, Facultade de Bioloxía, Universidade de Santiago de Compostela, 15706 Santiago de Compostela, Spain; *Author for correspondence*

Received 21 July 2000; accepted in revised form 15 January 2002

Key words: Acid-volatile sulfide, Pyrite, Salt-marsh soils, Sulfide, Trace metals

Abstract. In the present study, the pyritization of trace metals was studied in 12 soils from 3 salt marshes in the Ría of Ortigueira (NW Spain). The concentrations of trace metals in the pyrite fraction were related to physicochemical conditions, physiographical position in the salt marsh, and the presence or absence and type of vegetation. Redox conditions in soils from the low-salt marsh and from the creek bottom were strongly reducing throughout the profile, and there were higher concentrations of Fe and some trace metals (Cu and Mn) in the pyrite fraction (soluble in HNO_3) than in the reactive fraction (soluble in 1N HCl). In contrast, the trace-metal content in pyrite fraction in the surface layers of the high-salt marsh was low. In some of the soils, there was a significant increase in the pyrite content below 25 cm, and levels of Fe, Mn and Cu incorporated into this fraction were similar to those in the reactive fraction. The degree of pyritization varied greatly among metals in the order: Cu ~ Fe-1N HCl>dithionite-Fe>Ni ~ Mn>>Zn>Cr, although when we considered only the amorphous forms (ascorbate-Fe) as reactive-Fe, the order was: ascorbate-Fe>>Cu>Ni ~ Mn>>Zn>Cr. These differences appeared to be a consequence of the different geochemical behaviour of each metal (mainly in terms of the thermodynamic stability of sulfides and reaction kinetics), except for Zn. The low concentrations of Zn obtained may have been due to the solubility of ZnS in 1N HCl, which meant that it was extracted with the reactive fraction. Finally, we observed a direct relationship between DOP and DTMP, which was independent of the geochemical behaviour of each metal and of its concentration in the soil. Thus, the strong correlation between pyrite-Fe and the metals associated with this fraction appears to indicate that these metals coprecipitate with pyrite rather than form metal sulfides.

Abbreviations: AVS – Acid-Volatile Sulfide, DOP – degree of pyritization of Fe, DTMP – degree of trace-metal pyritization, dw – dry weight, MHWS – mean high-water springs, MLWS – mean low-water springs

Introduction

Since the beginning of the Industrial Revolution, large amounts of trace metals have been released into the environment, often affecting marine waters and sediments. Salt-marsh soils can act as both sources of, and sinks for, these contaminants, thus contributing to an increase or decrease in their concentrations in tidal flood waters (Valiela et al. 1976; Morse 1994). The main geochemical mechanisms by which heavy metals are retained in these soils are: adsorption by mineral and organic fractions, formation of complexes with organic ligands, and precipitation as insol-

uble forms (mainly as metal sulfides) or coprecipitation with authigenic mineral phases (Griffin et al. 1989; Huerta-Díaz and Morse 1992). In addition, flocculation and sedimentation of material in suspension are important routes of entry of metals into natural systems (Sager 1992).

Salt-marsh soils have been defined as having complex, three-dimensional patterns of alternating redox conditions (Wiegert et al. 1981). Previous studies carried out at the Ría of Ortigueira have shown that the soils present large spatial variations in their redox conditions, ranging from oxidizing (Eh > 300 mV) to strongly reducing (Eh < −100 mV) (Sánchez et al. 1998; Otero et al. 2000a). These variations can significantly affect speciation of trace metals. Under oxidizing conditions, trace metals are mainly associated with iron oxyhydroxides (Giblin et al. 1986; Griffin et al. 1989), whereas under reducing conditions, metals precipitate mainly as sulfides, or they coprecipitate with pyrite (Griffin et al. 1989; Huerta-Díaz and Morse 1992). Organic matter can also play an important role when the metals do not tend to form sulfides or when these are unstable, as with Cr (III) sulfide (Otero et al. (2000a, 2000b)).

A number of studies have been carried out concerning the Fe cycle and the biogeochemical processes that affect the formation of pyrite in the sea bed (e.g. Berner (1970) and Boesen and Postma (1988), Canfield et al. (1992), Wilkin and Barnes (1997), Canfield and Berner (1987), Huerta-Díaz and Morse (1990)), lakes and aquifers (Bottrell et al. 1995; Saunders et al. 1997; Huerta-Díaz et al. 1998), as well as in salt marshes (Howarth and Teal 1979; Howarth 1984; Howarth and Merkel 1984; Lord and Church 1983; Luther et al. 1991; Kostka and Luther (1994, 1995)). In contrast, few studies of trace-metal pyritization in salt-marsh soils have been carried out to date (Luther et al. 1980; Boulegue et al. 1982; Griffin et al. 1989; Huerta-Díaz and Morse 1992). Furthermore, in these studies, the number of soils examined was relatively low and the different geochemical conditions that can exist in a salt marsh were rarely considered.

We conducted a study of 12 soils from three salt marshes of the Ría de Ortigueira (NW Peninsula Ibérica), with the aim of establishing the spatial variation of the distribution of trace metals (Ni, Cr Cu, Mn, Zn) associated with the reactive (soluble in 1N HCl) and pyrite (soluble in HNO_3) fractions of the soils. The results are discussed in terms of (1) the physicochemical conditions of the soils, (2) the presence (or absence) and type of vegetation, (3) the physiographical position of the soils in the salt marshes and (4) the geochemical behaviour of each of the metals.

Materials and methods

Study area

The study area is located in the Ría of Ortigueira (NW Galicia, Iberian Peninsula), a relatively pristine area that has been designated as a wetland of international importance under the Ramsar Convention. Tidal periodicity is semi-diurnal with a

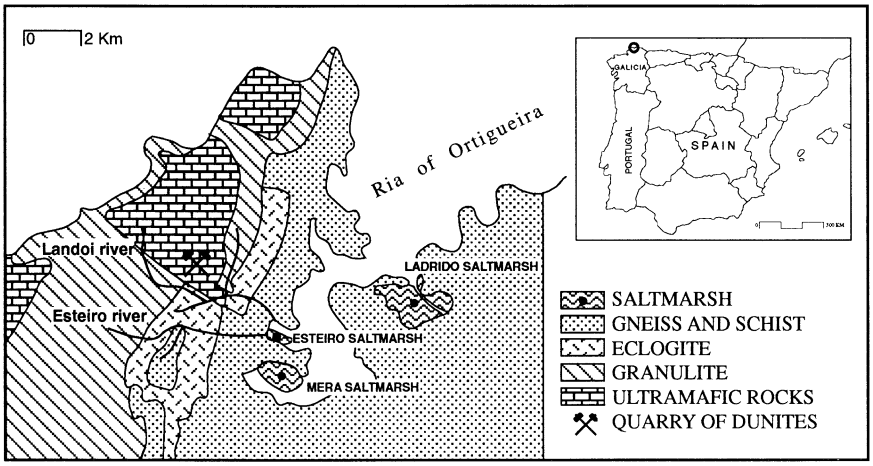

Figure 1. Map showing location and geology of the study area.

mesotidal range (3.6 m between MHWS and MLWS, Instituto Hidrográfico de la Marina (1993)). The substrate is comprised of gneiss and schists as well as basic (eclogite and granulite) and serpentinized ultrabasic rocks, the latter being characterized by having high concentrations of Cr and Ni (Van Calsteren 1978). There are a number of serpentinized periodite quarries in the area, one of which lies within the catchment area of the river Landoi, which flows into the Esteiro inlet (Figure 1). This quarry generates a waste sludge containing high levels of Cr (total Cr: 896.4 μg g^{-1}; Cr soluble in 1N HCl: 54.0 μg g^{-1}) and Ni (total Ni: 1690 μg g^{-1}, Ni soluble in 1 N HCl: 670.0 μg g^{-1}), which are transported via the river Landoi to the Esteiro salt marsh (Otero et al. 2000a). Previous studies have shown there to be great homogeneity in soil-particle size in the whole area, both spatially and at depth, with silty clay loam and silty clay textures predominating (Sánchez 1995; Otero et al. 2000a; Otero 2000).

Sampling and analysis of soils

Soil sampling was carried out in March 1996 at the different physiographical positions in the Esteiro, Mera and Ladrido salt marshes, as shown in Figure 1 and Table 1. Core samples were collected at low tide using PVC tubes, (diameter, 11 cm length, 35 cm). Tubes were hermetically sealed and transported in a vertical position to the laboratory where they were frozen at −18 °C, cut into 5 cm sections with a carbon-fiber saw and replaced in the freezer until use. Redox potential (Eh) and pH were determined *in situ* with a Solomat 2000 instrument previously calibrated – for Eh measurements – using a redox solution (Crison, Eh:468±5 mV at 25 °C) and – for pH measurements – using two buffer solutions of pH 4 and pH 7. The value obtained was then corrected by adding the potential of a calomel reference electrode (244 mV). Organic carbon was determined using a LECO model

Table 1. General characteristics of the different sampling sites (after Otero (2000)).

	Type of salt marsh	Physiographical position	Dominant plant species	Characteristic Soil
ESTEIRO				
EST1	Low-or pioneer salt marsh	Marsh flat	*Spartina maritima*	Typic Sulfaquents
EST2		Creek edge	*Spartina maritima*	Typic Sulfaquents
EST3		Creek bottom	No vegetation	Typic Sulfaquents
MERA				
MERA1		Hollow	*Spartina maritima*	Typic Sulfaquents
MERA2	High-salt marsh	Creek edge	*Halimione portulacoides*	Salic Hydraquents
MERA3		Creek bottom	No vegetation	Typic Sulfaquents
MERA4		Marsh flat	*Juncus maritimus*	Salic Hydraquents
MERA5		Back marsh	*Scirpus maritimus*	Histic Sulfaquents
MERA6				
LADRIDO				
LAD1	High salt marsh	Hollow	*Spartina maritima*	Typic Sulfaquents
LAD2		Creek edge	*Spartina maritima*	Salic Hydraquents
LAD3		Salt pan	No vegetation	Salic Hydraquents

CNS-1000 after removing the carbonates present with 6N HCl (Huerta-Díaz and Morse 1992).

The concentration of acid-volatile sulfides (AVS) was determined in triplicate using the method of Kostka and Luther (1994). Sulfide was released from AVS in the wet sample (0.25–1 g) by adding 20 ml of previously deaerated 6N HCl for 40–50 min in a gas-tight reaction flask through which nitrogen was bubbled. The H_2S released was transferred by the flow of nitrogen to another reaction flask containing 25 ml of 3% Zn acetate, to which 1 ml of concentrated H_2SO_4 and 4 ml of diamine B reagent were added (Kostka and Luther 1994). The concentration of sulfide was then colorimetrically determined with a UV-VS spectrophotometer at 670 nm according to the methylene blue method of Cline (1969). Test solutions ($Na_2S{\cdot}9H_2O$ in deaereated water) were prepared daily and the percentage of recovery was greater than 92%. The limit of detection was 0.02 μmol g^{-1}, established as 2.5 times the standard error of the blank (Bruland et al. 1979).

Reactive-Fe, the fraction of Fe that can react with sulfides to form pyrite (Berner 1970), was extracted with the citrate-dithionite method used in previous studies and which can also be used to extract amorphous and crystalline iron oxyhydroxides and AVS (see e.g. Kostka and Luther (1994, 1995)). The extraction was carried out in triplicate by using a 0.5 g wet sample, following the method established by Ko-

stka and Luther (1994). The degree of Fe pyritization (DOP), a term proposed by Berner (1970), was calculated in order to establish the percentage of reactive iron incorporated into the pyrite fraction. The calculation was made using Equation (1), assuming reactive-Fe to be that extracted with dithionite (DOP-dithionite), according to the recommendations of Raiswell et al. (1994).

$$DOP(\%) = ((\text{pyrite} - Fe)/(\text{pyrite} - Fe) + (\text{Reactive} - Fe)) \times 100 \quad (1)$$

In addition, we calculated the degree of Fe pyritization by considering only the amorphous forms of Fe and AVS-Fe as reactive-Fe, thereby reflecting the idea concerning the reactivity of the different forms of Fe in recent diagenetic processes, as explained in previous studies (see e.g. Postma and Jakobsen (1996)), and which may affect the incorporation of trace metals in the pyrite fraction (see e.g. Morse and Luther (1999)). Amorphous iron oxyhydroxides were also extracted with the method proposed by Ferdelman (1988), using sodium ascorbate-citrate buffered to pH 8 with sodium bicarbonate. The extraction was carried out in triplicate using a 0.5 g wet sample, to which was added 10 ml of ascorbate mixture for 24 h at room temperature, while shaking at 125 rpm (Kostka and Luther 1994). Finally, in order to make comparisons with the previous two extractions and the results of previous studies, the DOP levels were calculated for some of the soils (MERA1, MERA3, EST1, EST2, EST3, LAD1, LAD2, LAD3) by considering the iron soluble in 1N HCl as the reactive-Fe. For this, we used the method of Huerta-Díaz and Morse (1990), explained in further detail below. Extraction of iron with cold 1N HCl is less specific than extraction with dithionite or ascorbate, dissolving mainly armorphous and crystalline forms of Fe, except goethite and hematite, as well as large quantities of Fe associated with silicates and AVS-Fe (see e.g. Raiswell et al. (1994) and Kostka and Luther (1994)).

Trace metals and iron associated with the operationally defined reactive phase as well as trace metals associated with the pyrite phase were determined in triplicate using the sequential-extraction method of Huerta-Díaz and Morse (1990). Briefly, the method consists of the extraction of four operationally defined fractions: (1) reactive, consisting essentially of metals associated with carbonates and Fe and Mn oxyhydroxides, extracted with 20 ml of 1N HCl during 16 h of continuous shaking; (2) silicate, consisting essentially of metals associated with clays and other aluminosilicates, extracted with 30 ml of 10 M HF during 16 h of continuous shaking; (3) organic, consisting essentially of metals associated with organic matter, extracted with 10 ml of concentrated H_2SO_4 during 2 h of continuous shaking; and (4) pyrite, consisting essentially of metals associated with pyrite, extracted with 10 ml of concentrated HNO_3 during 2 h of continuous shaking. More recently, Cooper and Morse (1998) have shown that HNO_3 is an efficient extractor of other sulfide metals that also appear in sediments (e.g. CuS, CuS_2).

The degree of trace-metal pyritization (DTMP), a term proposed by Huerta-Díaz and Morse (1990) and which gives an estimation of the amount of a particular metal (Me) incorporated into the pyrite phase, was calculated using the following equa-

tion:

$$DTMP(\%) = ((\text{Pyrite} - Me)/(\text{Pyrite} - Me) + (\text{Reactive} - Me)) \times 100 \qquad (2)$$

General analytical procedures

Laboratory and field equipment used during collection and analysis of samples was soaked in a solution of 20% HCl overnight and was then rinsed twice with distilled water and Milli-Q water. The concentrations of Cr, Ni, Cu, Mn, Fe and Zn in each extract were determined by flame-atomic-absorption spectrophotometry (Perkin-Elmer model 1100B). The concentrations were always expressed in terms of dry weight of soil (dw), the moisture content being determined from two subsamples dried at 105 °C to constant weight.

Statistical analysis

The relationships between Fe and metals associated with the pyrite phase were determined by calculating Spearman's coefficients of correlation. All analyses were carried out using a SYSTAT 5.0 computer programme (Systat INC 1992).

Results

General characteristics of the soils

The general characteristics of the soils are shown in Table 2. There was a large variation in the percentage of total organic carbon (1.3–25.7%). The highest values were found in soils colonized by a monospecific stand of *Scirpus maritimus* (MERA5 and MERA6) (10.2–25.7%) and the lowest in the soil from the salt pan (3.8–1.3%, soil LAD3). Field pH ranged from 5.4 (MERA4, at a depth of 2.5 cm) to 7.2 (MERA1, 22.5 cm depth), with values from 6 to 7 being most common; the pH of the interstitial water of these soils was higher, ranging from 7 to 8 (data not shown; Otero (2000)). Differences in the redox status were particularly notable in the surface layers of the soils, with oxidized (Eh > 300 mV; e.g. MERA2, MERA4), suboxic (Eh 100–300 mV; e.g. MERA1; LAD2; MERA5) and reduced (Eh < 100 mV and high concentrations of AVS; MERA3, EST2, EST3, LAD1) environments being found. Most of the soils tended to become more reduced with depth. In general, the most reduced environments were found in the soils from the low-salt marsh (EST2: Eh = −90 mV and EST3: Eh = −26 mV, 2.5 cm depth). There were large variations in the redox potentials in the high-salt marsh, from Eh = −150 mV in MERA3 soils (creek bottom) to 450 mV in MERA4 (marsh flat) colonized by rushes (mainly *Juncus maritimus*). High values were also obtained at the edges of the creek (MERA2), occupied by *Halimione portulacoides* (Eh = 331 mV at 2.5

cm depth). Although in most of the soils conditions tended to become more reducing with depth, there were exceptions, such as those of the high-salt marsh situated at the creek edge (MERA2, LAD2) and the marsh flat (MERA4) where conditions were predominantly oxidizing.

Spatial variations in concentrations of AVS and variations with depth are shown in Figure 2, which clearly illustrates the substantial differences between soils. The highest values were found in the surface layers of the low-salt marsh but with a range of values between 47.3±5.90 μmol g^{-1} for EST1 (marsh flat) and 4.00±1.40 μmol g^{-1} for EST3 (creek bottom). In the high-salt marsh, the highest concentrations were found in the superficial layers of soils in areas not colonized by vegetation, such as the creek bottom (MERA3: 9.60±3.00 μmol g^{-1}) and the salt pan (LAD3: 20.2±6.30 μmol g^{-1}). Relatively high concentrations were also found in the surface layers (2.5 cm depth) of the soils colonized by *Spartina maritima* (MERA1: 10.50±3.60; μmol g^{-1}, LAD1 13.02±3.30 μmol g^{-1}). In these soils, the concentration of AVS decreased with depth, in an irregular way. The concentrations of AVS were very low between depths of 2.5 cm and 15 cm, where roots and rhizomes are most dense (Otero 2000). A new peak was then reached at a depth of 17.5 cm, with concentrations similar to those found in the surface layers. In the remaining soils from the high-salt marsh, the concentrations of AVS were very low throughout the profile, with the highest values appearing below 20 cm, as in sites colonized by *Scirpus maritimum* (MERA5: 14.30±1.5 μmol g^{-1}, MERA6: 9.10±2.4 μmol g^{-1} at 27.5 cm). The lowest values were found in the areas of the marsh flat colonized by rushes (MERA4) and at the creek edge (MERA2, LAD2), where the values of AVS in most of the soil profiles were below the limit of detection.

Reactive and Fe-pyrite

In general, high concentrations of dithionite-Fe were found in the superficial layers of the soils (0–10 cm), the highest values corresponding to MERA5 and MERA6 samples (MERA5: 3400±400 μmol g^{-1} and MERA6: 995±175 μmol g^{-1} at a depth of 2.5 cm; Figure 3). High values were also found in the soils from the high-salt marsh flats (MERA1: 450±18.0 μmol g^{-1}, MERA4: 480±40.0 μmol g^{-1}, at 2.5 cm depth), as well as the creek bottom (LAD2 462±31.9 μmol g^{-1} and MERA2: 400±34.0 μmol g^{-1}, at 2.5 cm depth). The concentrations of dithionite-Fe in the surface layers of the low-salt marsh (Esteiro) soils were markedly lower than in the high-salt marsh soils, ranging between 310±37.0 μmol g^{-1} in EST2 (creek edge) and 261±38.1 μmol g^{-1} in EST2 (marsh flat). The lowest values in surface layers were found in the salt pan (LAD3: 86.6±16.1 μmol g^{-1}), but the values increased with depth until a maximum of 240±17.0 μmol g^{-1} was reached in the deepest part of the soil (22.5 cm).

The concentration of Fe associated with the pyrite fraction was generally low in surface layers but increased with depth, in some cases reaching higher concentrations than those of the reactive-Fe (e.g. EST1, EST2, EST3, MERA1, LAD1, LAD2; see Figure 3). The highest concentrations were found in the low salt marsh (EST1: 90.2±5.30–586±27.6 μmol g^{-1}; EST2: 320±30.0–107±7.60 μmol g^{-1} and

Table 2. General characteristics of the Ría of Ortigueira salt-marsh soils.

Depth (cm)	Esteiro salt marsh			Mera salt marsh						Ladrido salt marsh		
	EST1	EST2	EST3	MERA1	MERA2	MERA3	MERA4	MERA5	MERA6	LAD1	LAD2	LAD3
TOC (Total Organic Carbon) (%)												
2.5	7.6	5.6	2.3	7.6	5.6	3.2	10.5	22.6	24.8	5.5	4.3	3.8
7.5	6.0	5.1	2.1	7.1	6.0	2.5	12.6	25.2	25.7	5.0	4.4	3.5
12.5	5.7	4.0	1.8	9.2	5.6	2.6	8.5	22.7	21.8	4.2	4.0	3.1
17.5	6.8	4.0	1.2	8.9	5.1	2.0	7.7	18.4	15.0	4.8	5.4	1.6
22.5	6.9	3.8	nd	7.3	5.6	2.6	5.9	14.3	11.5	5.5	4.3	1.3
27.5	6.9	3.7	nd	7.4	3.6	2.5	4.1	nd	12.4	5.7	6.9	nd
32.5	4.3	3.7	nd	6.6	4.5	2.1	3.0	nd	10.2	5.2	7.0	nd
Field pH												
2.5	6.5	6.6	7.6	6.6	6.6	6.3	5.4	6.5	6.4	6.5	6.3	6.6
7.5	6.1	6.3	7.5	6.4	7.1	6.3	5.6	6.2	nd	6.3	6.4	6.7
12.5	6.5	6.7	7.8	6.4	7.2	6.3	6.4	6.3	6.4	6.5	6.3	6.5
17.5	6.5	6.5	7.9	7.2	7.7	5.8	6.6	6.5	nd–	6.6	6.2	6.7
22.5	nd	6.5	nd	6.5	7.1	5.7	6.6	6.5	nd	6.7	6.1	nd
27.5	nd	nd	nd	nd	7.7	6.1	nd	nd	nd	nd	nd	nd
32.5	nd	nd	nd	nd	7.2	5.9	nd	nd	nd	6.7	nd	nd
Redox potential (mV)												
2.5	60	−85	−26	90	331	−150	420	353	94	−26	211	−15
7.5	−80	−135	−10	20	340	−189	410	84	nd	−3	279	−53
12.5	3	−155	−98	−103	340	−167	420	nd	nd	−50	169	87
17.5	−95	−170	nd	−100	92	−187	407	−188	−27	−125	206	56
22.5	−115	−180	nd	−150	146	−178	360	nd	nd	nd	141	nd
27.5	−250	−225	nd	−166	nd	−190	nd	nd	nd	−160	nd	nd
32.5	nd	−250	nd	nd	nd	−175	nd	nd	nd	nd	nd	nd

nd: no data available

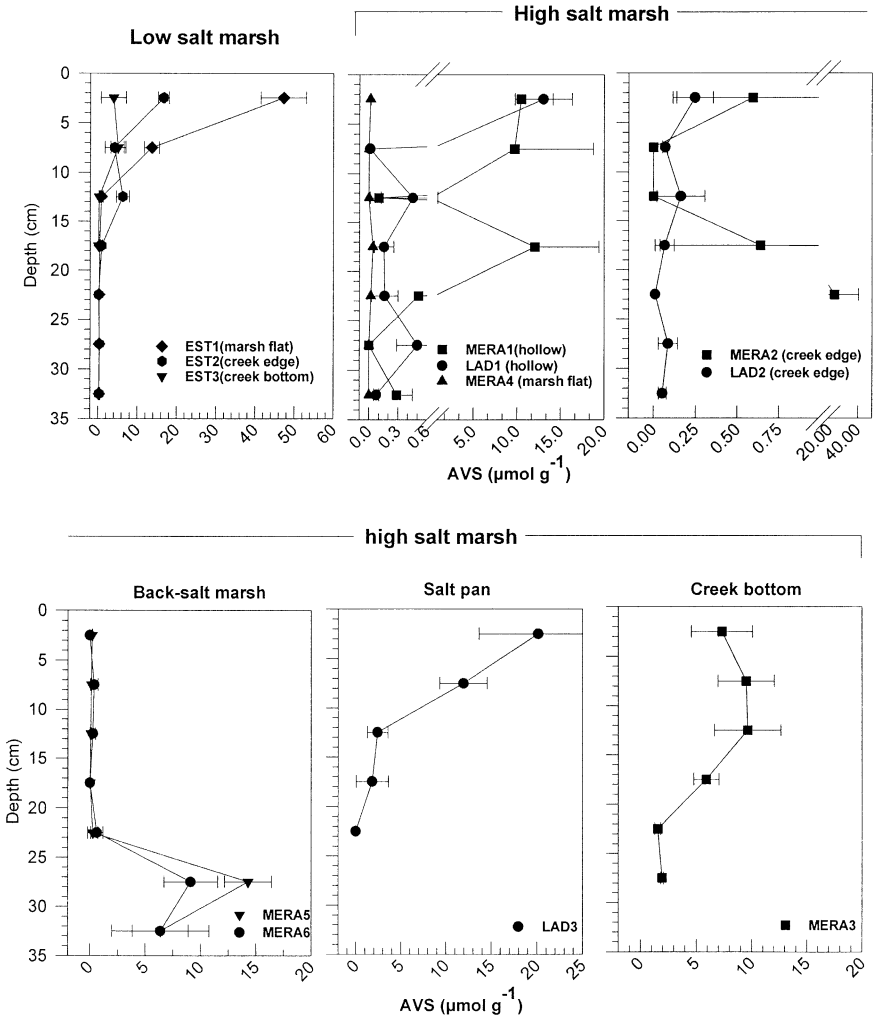

Figure 2. Spatial variation in the concentration of acid-volatile sulfide (AVS). Horizontal bars represent the standard deviation.

EST3: 41.0±1.53–227±45.0 μmol g^{-1}), with the pyrite-Fe in EST2 always being higher than the dithionite-Fe. In the high-salt marsh, the concentrations of pyrite-Fe were generally lower than those found in the low-salt marsh. The highest concentrations occurred in the environments whose topographical positions meant that they were subjected to longer periods of flooding, such as the creek bottom (MERA3: 166±10.2–212±15.3 μmol g^{-1}), hollows (MERA1: 23.7±11.9–470±30.1 μmol g^{-1} and LAD3: 0.25±0.10–103±3.70 μmol g^{-1}) or the back-marsh (MERA5: 8.32±3.1–303±36.7 μmol g^{-1} and MERA6: 4.70±0.80–450±58.3 μmol g^{-1}). In contrast, the concentrations in well-drained areas such as the creek edge or the marsh flat were

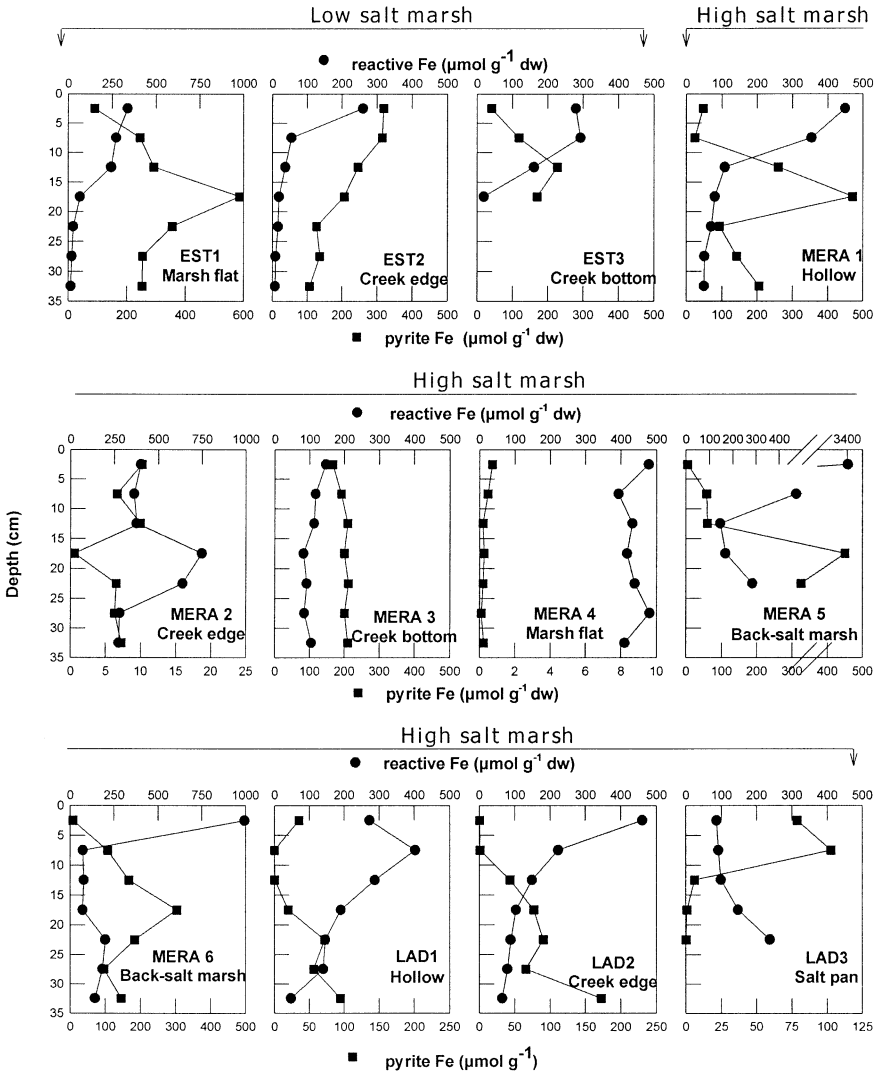

Figure 3. Spatial variation in concentration of reactive and pyrite-Fe. Note the different scales used.

much lower (MERA2: 0.60±0.16–10.0±0.4 μmol g^{-1}, MERA4: 0.11±0.03–0.73±0.1 μmol g^{-1}).

Trace metals associated with the reactive and pyrite fractions

The concentrations of Ni, Cr, Mn, Cu and Zn in the reactive and pyrite fractions are shown in Figures 4, 5, 6, 7 and 8, respectively. There were high levels of Ni (EST2: 5740±370 nmol g^{-1}, ~340 μg g^{-1}, 2.5 cm depth) and of Cr (EST2: 1600±140 nmol g^{-1}, ~83.2 μg g^{-1}, 2.5 cm depth) in the reactive fraction of the

upper 10 cm of the Esteiro salt-marsh soils. These soils also contained a large amount of Ni incorporated into the pyrite fraction (EST2: Ni 2640±190 nmol g^{-1}, $\sim$166 μg g^{-1}, at 2.5 cm), but not of Cr, which was always found at very low concentrations in the pyrite fraction (maximum concentration: EST1: 67.1±9.5 nmol g^{-1}, 3.50 μg g^{-1} at 7.5 cm depth). The concentrations of reactive-Mn were quite varied; the highest values were primarily found in the surface layers of each soil, and ranged from 6860±2300 nmol g^{-1} in the MERA6 soil to 444.5±75.0 nmol g^{-1} in the LAD3 soils. The pyrite-fraction concentration was generally lower than the reactive fraction, except in strongly reduced low-salt marsh soils, in which the concentration of the pyrite fraction was higher than that of the reactive fraction (below 2.5 cm) (Figure 6). The concentrations were highest in the EST2 soils (2490±310 nmol g^{-1} at 7.5 cm depth) and lowest in the MERA 4 soil, where they were also below the limit of detection (0.38 nmol g^{-1}). The concentration of reactive-Cu varied between 5.20 nmol g^{-1} in the deepest part of the EST2 soil and 650 nmol g^{-1} in MERA5, and that of the pyrite between 3.10±1.00 nmol g^{-1} in MERA2 and 457±60.0 nmol g^{-1} in MERA5. The results show that pyrite-Cu constitutes an important part of these soils, and is often present at concentrations similar to or even higher than those of the reactive fraction (e.g. EST1, EST2, MERA1, MERA3, LAD1). In contrast, relatively low concentrations of Zn were found in the pyrite fraction, in many cases below the limit of detection (2.40 nmol g^{-1}), and much higher concentrations ranging between 100 nmol g^{-1} and 1100 nmol g^{-1} were found in the reactive fraction (Figure 8).

In addition, there was a strong correlation between the concentration of pyrite-Fe and the metals associated with this fraction (Cr: r_s=0.523; Zn: r_s = 0.756; Cu: r_s = 0.896; Mn: r_s = 0.844; Ni: r_s = 0.880; $P < 0.001$ in all cases and n = 77 except for Zn, where n = 33) (Figure 9).

Degree of pyritization of Fe (DOP) and trace metals (DTMP)

Figure 10 shows the degree of Fe pyritization, in terms of Fe soluble in dithionite (DOP-dithionite), plotted against the degree of trace-metal pyritization (DTMP). The highest levels of Fe pyritization were found in the low-salt marsh soils; values ranged from 21–95%, increasing gradually with depth. The high-salt marsh soils gave more varied results, with DOP-dithionite values ranging from less than 1% (e.g. MERA4) to greater than 80% (e.g. MERA1); again, the highest levels were found in the deeper layers of the soils. The DOP-ascorbate showed that there was almost total pyritization of the amorphous forms of Fe in the low-salt marsh soils, with values ranging from 48–100%, but most commonly in the 85–100% range (Figure 11).

Regarding the pyritization of trace metals, it was found that Cu showed the highest degree of pyritization, which was greater than 95% in the EST1, EST2 and MERA3 soils (Figure 10). The degree of pyritization of Mn ranged from 0–85%, and was followed in descending order, by Ni (0.3–45%), Zn (0–45%) and Cr (0.25–16%). If we consider the response of the DTMP to increasing DOP-dithionite, we can distinguish at least three different types of behaviour. Firstly, there was

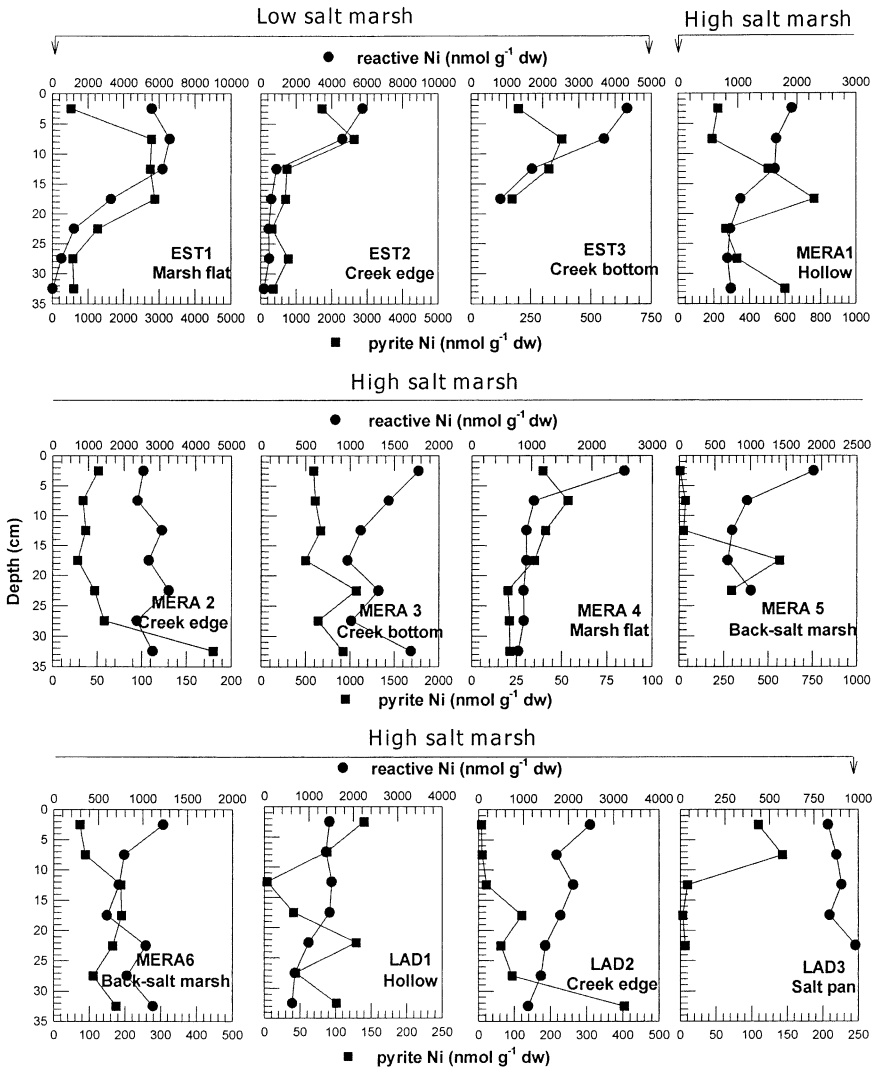

Figure 4. Spatial variation in concentration of reactive and pyrite-Ni. Note the different scales used.

a gradual and significant increase in DTMP of Cu with increasing DOP-dithionite. Secondly, there was a significant increase in the degree of pyritization of Mn and Ni from values of DOP-dithionite above 50%. Finally, the increase in the degree of pyritization of Zn and Cr, with increasing DOP, was very low (generally no more than 20% and 10%, respectively). However, when only the amorphous forms of Fe (ascorbate-Fe) were considered, it was found that the highest degree of trace-metal pyritization was produced at DOP-ascorbate levels above 80% (Figure 11).

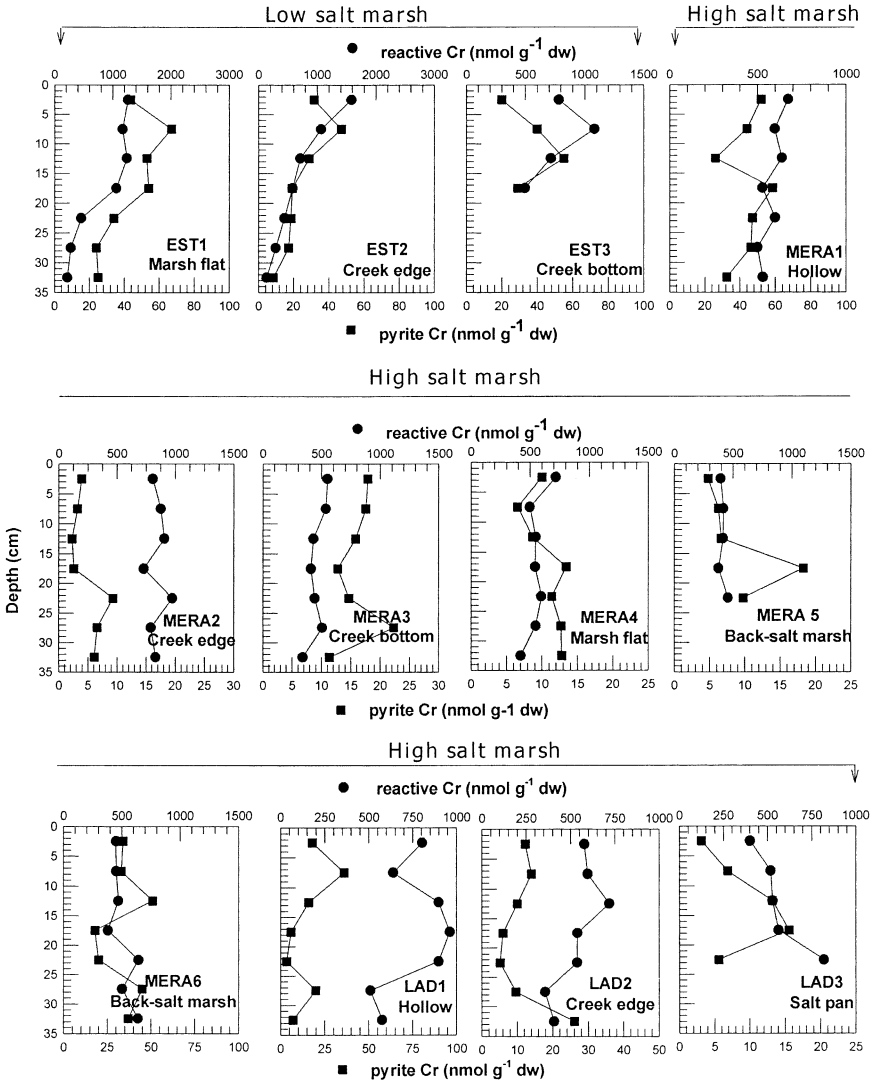

Figure 5. Spatial variation in concentration of reactive and pyrite-Cr. Note the different scales used.

Discussion

Trace metals in reactive and pyrite fractions in relation to changes in physiography and vegetation

It has been pointed out in different studies that salt-marsh soils can show large spatial variations in their geochemical conditions due to differences in physical factors (influence of tides, drainage, physiographical changes, etc.) and/or biotic factors

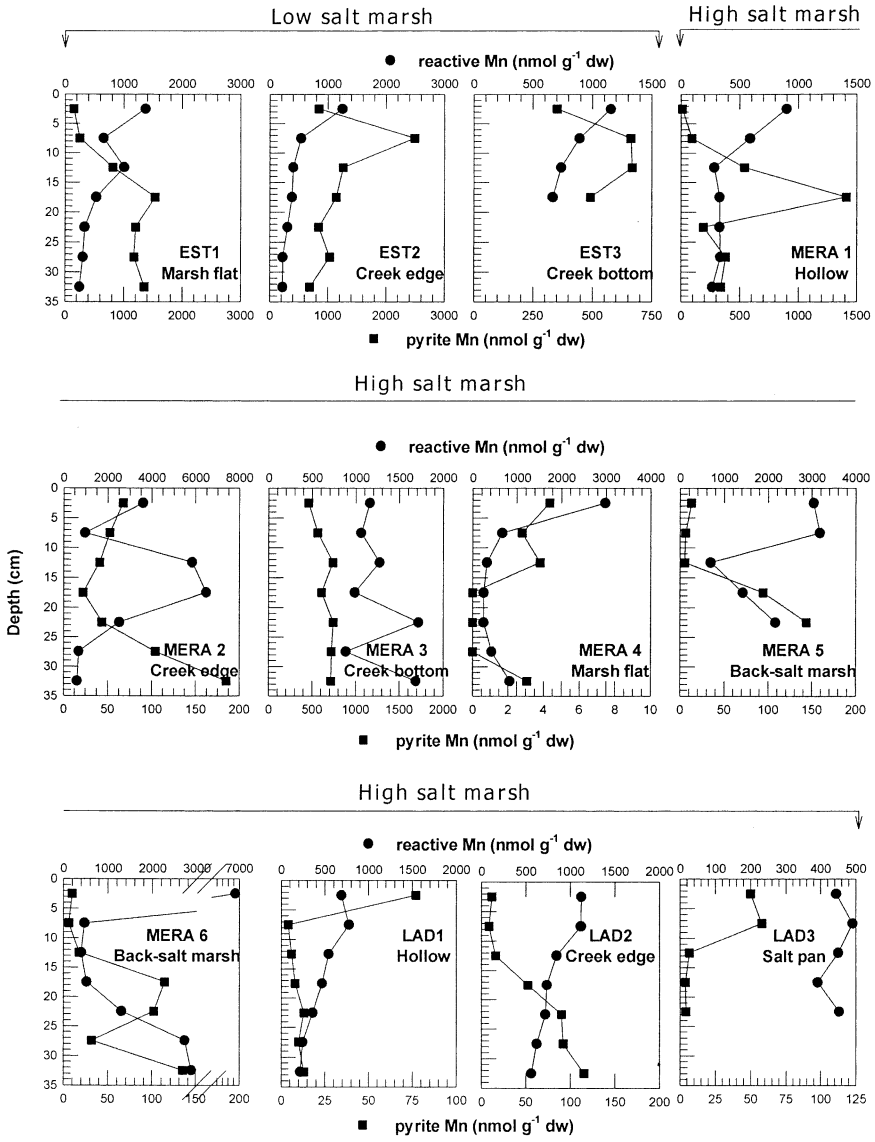

Figure 6. Spatial variation in concentration of reactive and pyrite-Mn. Note the different scales used.

(bioturbation, microbial activity, etc.) (see e.g. Howes et al. (1981) and Gardner et al. (1988)). These changes can affect the speciation of trace metals in the soils as well as their bioavailability. The results obtained in the present study were in agreement with this idea, and showed highly varied geochemical conditions – as illustrated by the pH (5.5–7.9), redox potential (–250 to 420 mV) and concentration of AVS (<0.02–57.4 μm g^{-1}) (Figure 2, Table 2). In accordance with these variations, there were large differences among soils as regards the heavy metals

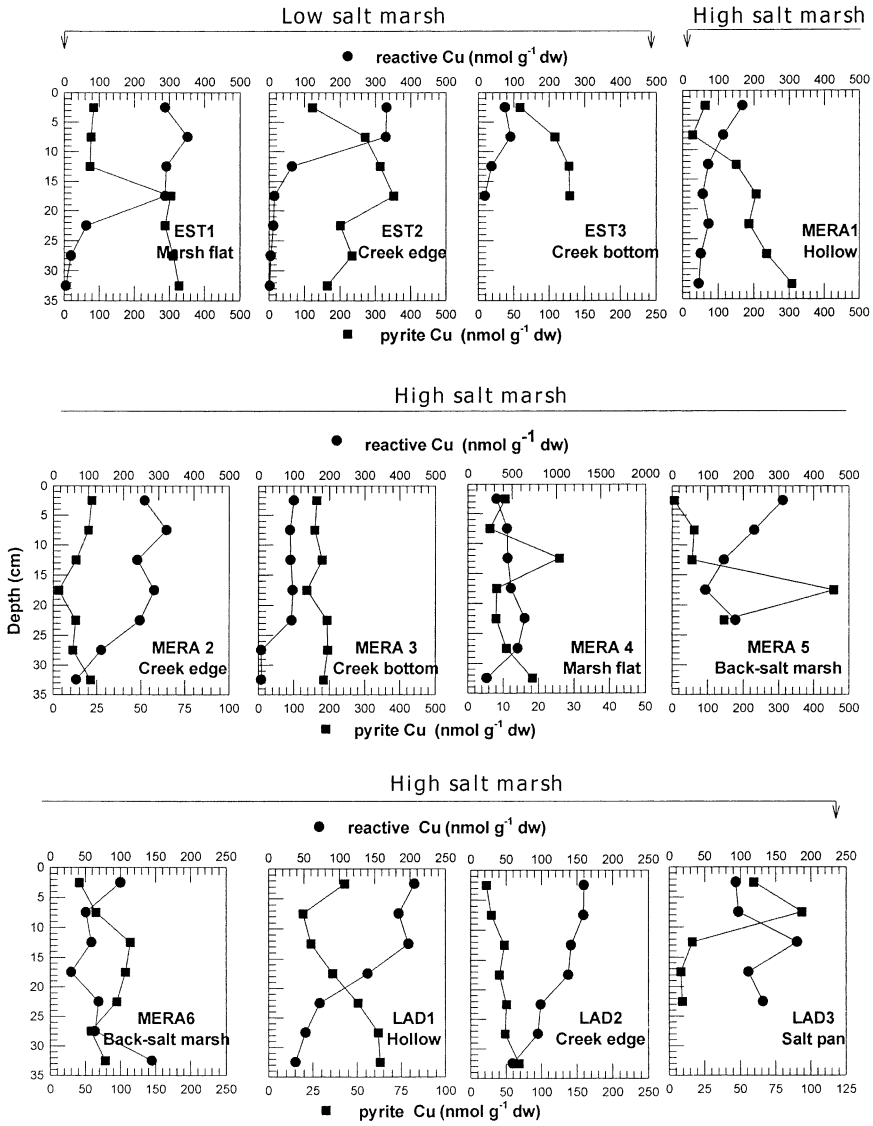

Figure 7. Spatial variation in concentration of reactive and pyrite-Cu. Note the different scales used.

associated with the reactive and pyrite phases (Figures 3, 4, 5, 6, 7 and 8). In general, the metals contained in salt marshes are mainly associated with the reactive fraction (presumably iron and manganese oxyhydroxides). Previous studies have already demonstrated the important role of iron and manganese oxyhydroxides in the adsorption and coprecipitation of heavy metals in soils (e.g. Jenne (1968) and Schoer (1985), Khawary et al. (1992)). The lowest concentrations of metals associated with the pyrite fraction were found at the creek edge, colonized by *Halimi-*

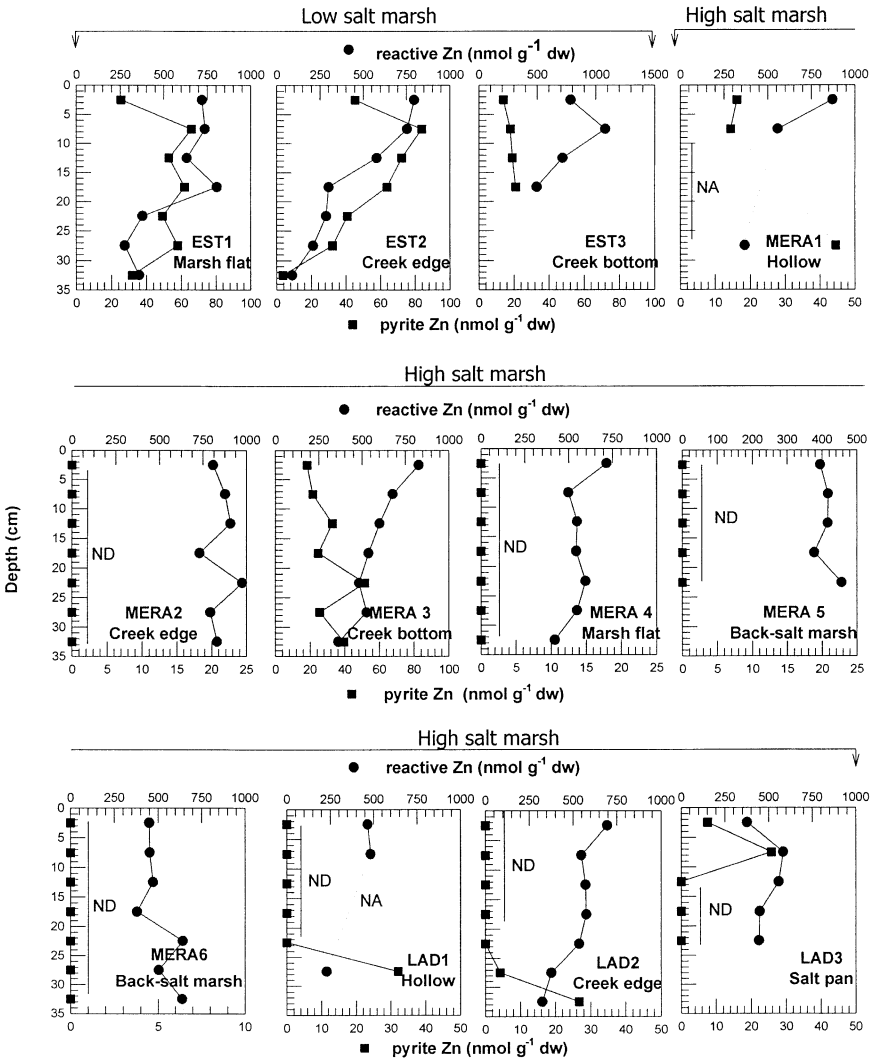

Figure 8. Spatial variation in concentration of reactive and pyrite-Zn. Note the different scales used. NA: not analysed, ND: not detected.

one portulacoides (MERA2) and in the area colonized by rushes (MERA4), because the lowest concentrations of pyrite were formed here. Previous studies have indicated that *H. portulacoides* occupies the edges of the creeks because they require well aerated soils for growth (Russell et al. 1985; Sánchez et al. 1998). Low concentrations of metals associated with the pyrite fraction were also found in the surface layers of the soils from the creek edge in the Ladrido salt marsh (LAD2) and in the low-salt marsh (EST1). The soils at these sites are better aerated than others because of the greater water flow at the creek edges, which increases their

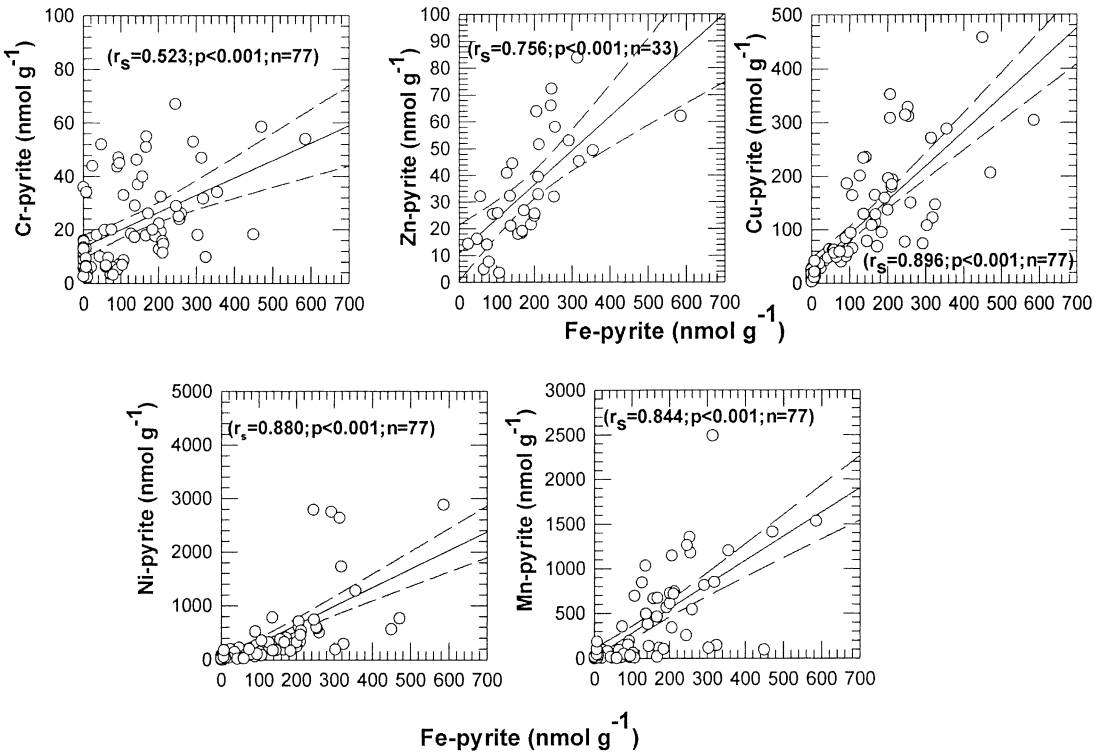

Figure 9. Relationship between pyrite-Fe and Cr, Zn, Cu, Mn and Ni associated with pyrite fraction. Dotted lines represent the 95% confidence interval.

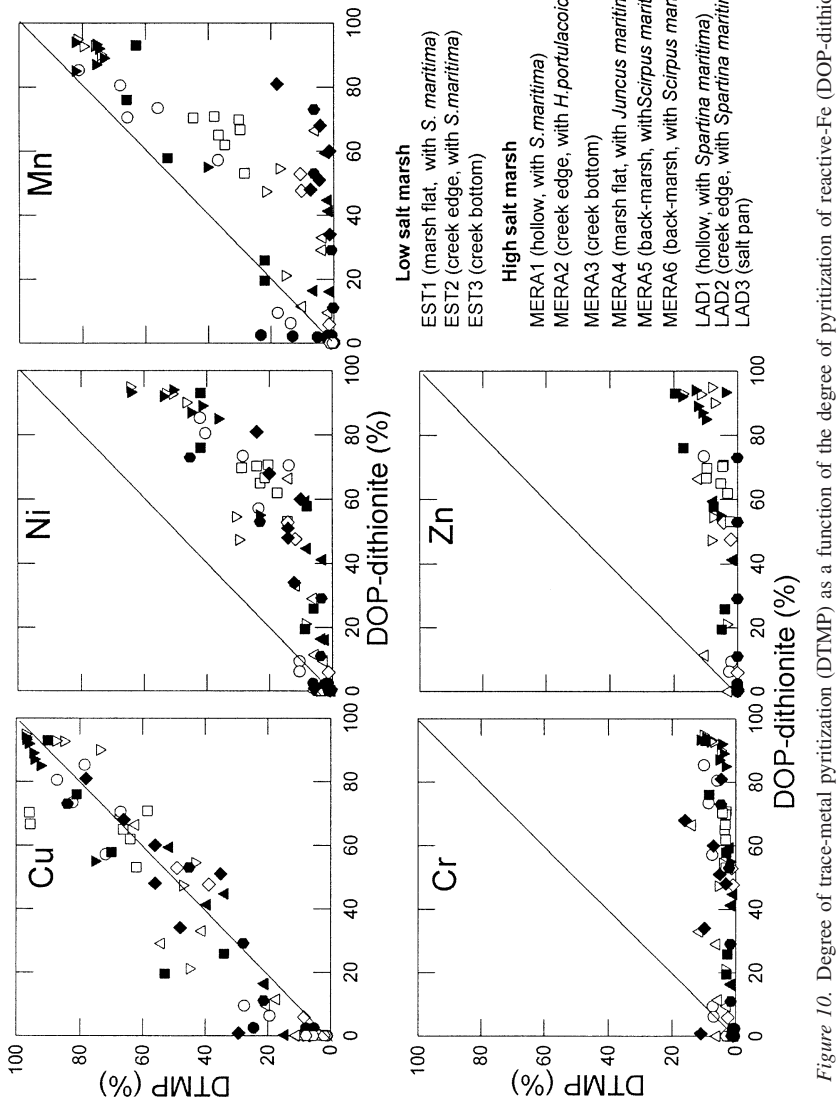

Figure 10. Degree of trace-metal pyritization (DTMP) as a function of the degree of pyritization of reactive-Fe (DOP-dithionite).

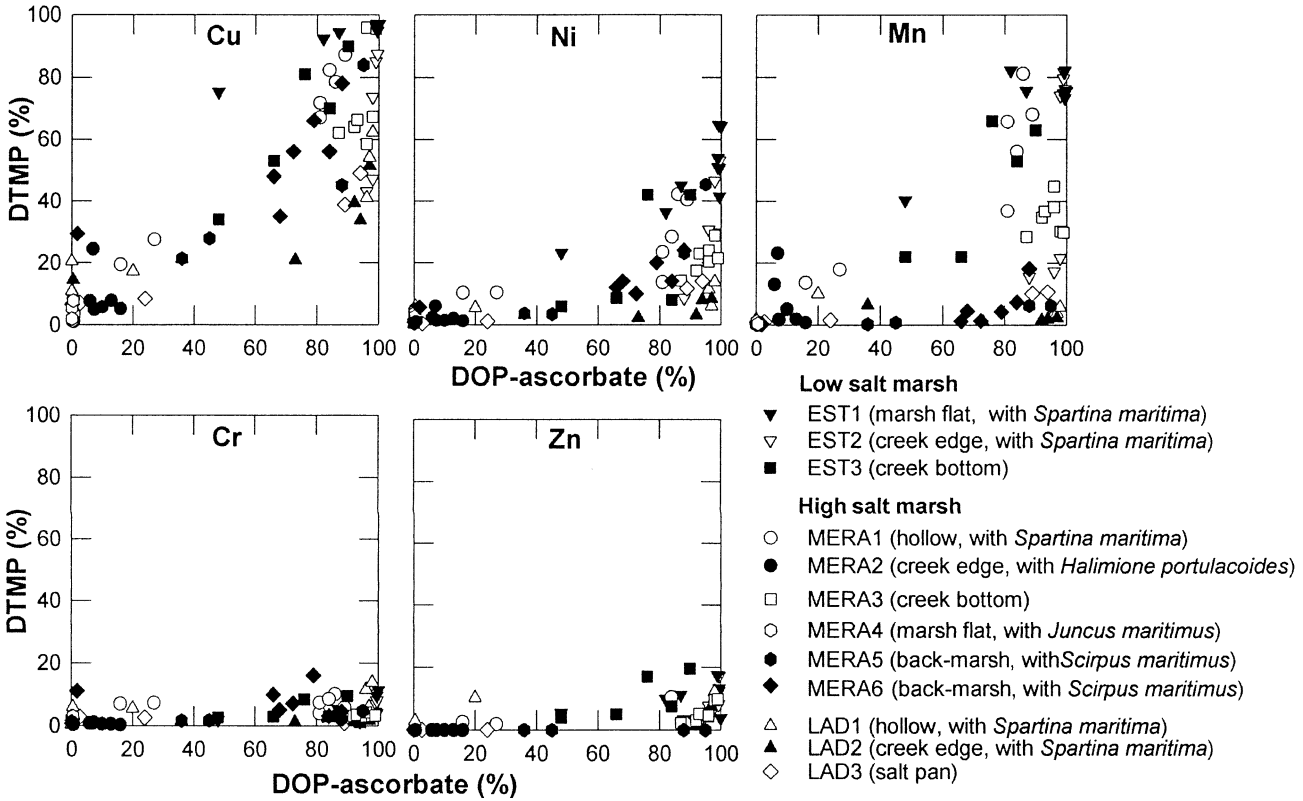

Figure 11. Degree of trace metal pyritization (DTMP) as a function of the degree of pyritization of reactive-Fe (DOP-ascorbate).

drainage (Jordan 1985; Price et al. 1988). The activity of crabs (mainly the construction of burrows) at the creek edges also contributes significantly to soil aeration (Gardner 1990). Rushes (*Limonio-Juncetun maritimae* community) occupy wide areas of the marsh flats and are situated at heights ranging from 304–390 cm, in some parts higher than the mean high-tide level (376 cm; Sánchez et al. (1996)). In this case, the low concentrations of AVS and of metals associated with the pyrite phase may be due to a number of factors. On one hand, despite being one of the most frequently flooded areas (Sánchez 1995), its flat formation allows effective drainage of the tidal water, so that the periods of flooding are not prolonged. Furthermore, in a study conducted at this salt marsh, at monthly intervals over a one year and a half period Sánchez (1995) found that the water table is relatively low during low tide (at a depth of 15.9±2.8 cm).

The plant community made up of *Scirpus maritimus* is found at higher levels than the previously mentioned species (377±10.0 cm), and is thus less frequently flooded (Sánchez 1995). However, the soils here had a higher content of metals associated with the pyrite fraction and AVS, especially below a depth of 20 cm. The data recorded by Sánchez (1995) shows that the water table at this site is very close to the surface (at a depth of 2.8±4.1 cm), possibly due to run-off from the land as well as emergence of fresh water from the water table itself. The latter idea is supported by the low electrical conductivity registered in the soils (3.9±4.1 dS m^{-1} in saturated extract; Otero (2000)) and in the water table (5.27±8.6 dS m^{-1}; Sánchez (1995)). However, in spite of the low electrical conductivity, the sulfate concentration found in the surface layers and at depth (16.21±5.2 mM at 0–10 cm and 24.80±7.8 mM at 10–30 cm; n = 11; Otero (2000)) was much higher than the concentration at which the rate of sulfate reduction may begin to slow down (1.6 mM; Van Cappellen and Wang (1996)). These unusually high sulfate concentrations may be a result of the oxidation of metal sulfides (mainly pyrite and AVS). Evidence supporting this idea is provided by the molar ratio of SO_4^{2-}/Cl^- (0.28±0.07 at 0–10 cm and 0.15±0.12 at 10–30 cm; n = 11), which was much higher than that found in seawater collected from the Ría de Ortigueira ($SO_4^{2-}/Cl^- = 0.05$, n=2) (Otero 2000). Compared with the previously mentioned soils, higher concentrations of metals associated with the pyrite fraction were found in the marsh flat of the low-salt marsh (EST2) and hollows of the marsh flat colonized by *S. maritima* (MERA1, LAD1), where the concentrations of some metals (Fe and Cu) were higher in the pyrite than in the reactive fraction. These results can be explained by the prolonged flooding of these soils resulting from poor drainage and a water table that is very close to the surface (at a depth of 0.2±0.8 cm; Sánchez (1995)).

The soils not colonized by vegetation (MERA3, creek bottom and LAD3, salt pan) were very different from each other. On one hand, the soil from the creek bottom (MERA3) was characterized by reducing conditions throughout the profile and by high concentrations of Fe and trace metals associated with the pyrite phase (which for Fe and Cu were higher than those associated with the reactive phase). On the other hand, the salt-pan soil (LAD3), which is permanently covered by water, was found to have reducing conditions in the upper 10 cm consisting of a greenish grey matrix (10Y4/1; according to the Munsell Color Company (1975))

with black mottles (5BG 2/1), presumably due the presence of Fe monosulfides – as reflected by the high concentrations of AVS (Figure 2); the concentration of pyrite-Fe was similar or even higher than that of the dithionite-Fe. However, below 15 cm, the redox potential was higher than in the surface layers; the concentration of the AVS and of the pyrite fraction decreased considerably, whereas the dithionite-Fe increased and the soil matrix was dark gray (5Y 4/1) with red mottles (5YR 4/6). We have no satisfactory explanation for these results because we did not find any factor that could limit sulfate reduction at depth. Thus, although the levels of TOC in the salt-pan soil were lower than in the other soils (Table 2), the concentration of DOC was similar or even higher than in other soils from this salt marsh without vegetation (i.e. LAD3, salt pan soil: 0–5 cm: 720 mg C l^{-1}; 20–25 cm.: 213 mg C l^{-1}; MERA3, creek bottom soil: 0–5 cm: 393 mg C l^{-1}, 20–25 cm: 86.4 mg C l^{-1}; data not shown), and the concentration of sulfate in the upper and lower parts of the soil was high and similar (19.2 mM at 0–5 cm and 18.1 mM at 20–25 cm; Otero (2000)). Furthermore, we did not observe any process (e.g. groundwater movement) that would cause fewer reducing conditions in the lower part of the soil than in the upper part.

Degree of pyritization of Fe (DOP) and trace metals (DTMP)

The degree of pyritization that we found in the Ortigueira salt-marsh soils was generally high and similar to that found in anoxic-sulfidic sediments (Table 3). The pattern observed for DTMP, which in descending order was Fe-1N HCl=Cu>>Mn>Ni>>Zn=Cr, was similar to that reported in previous studies carried out in different marine environments (Huerta-Díaz 1989; Huerta-Díaz and Morse 1992). The results obtained from the different methods used to extract Fe showed the DOP decreasing in the following order, ascorbate-Fe>>Fe 1N HCl>dithionite-Fe, and in some instances there was total pyritization of the non-crystalline forms of Fe (ascorbate-Fe) (Table 3). These results are in accordance with those of other authors who established that amorphous Fe is quickly incorporated into the pyrite fraction (Canfield et al. 1992; Kostka and Luther 1995).

Furthermore, our data also shows that pyritization of trace metals depends not only on their concentrations in the soil and the redox conditions of the soil but also on the geochemical behaviour of each metal. This is exemplified by the Ría of Ortigueira salt marsh soils. Previous studies have demonstrated that the Esteiro salt-marsh soils have high concentrations of non-residual Ni and Cr in the upper 10 cm as a result of contributions from a nearby serpentinized peridodite quarry (Otero et al. 2000a), and reducing conditions exist throughout the profile (Table 2). However, the DTMP of Cr was very low and similar to the values found for the Mera and Ladrido salt-marsh soils (Figures 5 and 10) and also to the values reported by Huerta-Díaz (1989) for other marine environments (Table 3). Chromium has a broad range of oxidation states (from −2 to +6), but only the +3 and + 6 are stable under most conditions of the surface environment (Fendorf 1995). Under suboxic or reducing conditions in salt-marsh soils, CrO_4^{2-} is reduced to Cr^{3+}, which, due to its electronic configuration [d^3, t_{2g}^3] is kinetically inert to reaction with sulfide

Table 3. Comparison of values of Degree of Iron Pyritization (DOP) and Degree of Trace Metal Pyritization (DTMP) obtained in the present study and in other studies from different marine environments. See Huerta-Díaz and Morse (1992) for more details of the different sites.

	DOP-Fe ascorbate %	DOP-Fe 1N HCl %	DOP-Fe dithionite %	DTMP-Mn %	DTMP-Cu %	DTMP-Ni %	DTMP-Zn %	DTMP-Cr %	Reference
Ortigueira salt marshes									
Average ± SD	58.4 ± 39.8	46.2 ± 29.4	40.5 ± 34.1	23.6 ± 28.5	45.4 ± 32.4	17.1 ± 17.5	4.30 ± 5.40	4.32 ± 3.5	Present study
Range	0.10–100	0.05–82.6	0.02–94.8	0.01–82.0	1.05–97.1	0.20–64.6	0.01–19.6	0.25–16.0	
Baffin Bay (n = 37)[a]									
Average ± SD	nd	66.5 ± 12.5	nd	29.2 ± 12.3	51.6 ± 25.9	47.0 ± 10.4	13.9 ± 2.7	8.2 ± 2.9	Huerta-Díaz (1989)
Range		26.9–82.3		4.0–49.0	18.4–99.6	22.2–64.1	7.5–18.5	1.9–15.8	
Atchafalaya Bay (n = 20)[b]									
Average ± SD	nd	15.4 ± 3.6	nd	0.62 ± 0.2	15.3 ± 4.9	17.3 ± 3.8	6.2 ± 1.5	13.6 ± 3.4	idem
Range		10.8–22.3		0.35–1.1	7.3–26.2	9.9–23.4	3.2–9.2	7.6–19.9	
Green Canyon (n = 16)[c]									
Average ± SD	nd	42.0 ± 21.6	nd	23.8 ± 12.8	81.3 ± 22.7	41.8 ± 13.3	8.4 ± 0.8	6.8 ± 2.5	idem
Range		1.8–62.0		0.3–35.6	41.1–100	17.7–54.2	7.1–10.0	3.7–12.3	
Orca Basin (n = 25)[d]									
Average ± SD	nd	4.9 ± 3.0	nd	0.7 ± 0.7	24.6 ± 4.1	16.5 ± 3.3	4.0 ± 0.9	7.2 ± 3.6	idem
Range		0.8–11.6		0.2–4.0	19.6–33.6	11.6–25.1	2.2–5.7	1.0–13.2	

Site: (a) anoxic-sulfidic coastal lagoon sediments; (b) anoxic-nonsulfidic delta sediments; (c) anoxic-sulfidic hemipelagic deep sediments; (d) euxinic hipersaline sediments. nd= no data available, n= number of samples; SD standard deviation

(Morse and Luther 1999), or if it does react, the resulting compounds are very unstable (Smillie et al. 1981). Moreover, it does not tend to coprecipitate with pyrite because prior to reaction with sulfide, the metals form hexaaquo complexes in solution, and Cr^{3+} has one of the slowest rate constants for water exchange in comparison with divalent metals (rate constant for water exchange: Cr: $\sim 10^{-6}$ sec^{-1}; Ni: 3×10^4 sec^{-1}; Fe: 3×10^6 sec^{-1}; Mn: 3×10^7 sec^{-1}; Zn: 3×10^7 sec^{-1}; Cu: 8×10^8 sec^{-1}; Burgess (1988)) (Morse and Luther 1999). Under reducing conditions in soils, Cr^{3+} tends to precipitate as insoluble chromium hydroxide (mostly as $Cr(OH)_3$) (Lu and Chen 1977; Sass and Rai 1987; Eary and Rai 1989), although high concentrations may also be found associated with organic matter (Guo et al. 1997; Otero et al. 2000a). Under oxidizing or suboxic conditions, Cr is mainly found associated with oxyhydroxides of Fe and Mn (Rai et al. 1989; Guo et al. 1997). Therefore under both reducing and oxidizing conditions in soils, high concentrations of Cr are found in the reactive fraction and low concentrations in the pyrite fraction. In contrast, Ni was gradually incorporated into the pyrite phase as the degree of pyritization of Fe (DOP) increased, but the DTMP was always less than the DOP. This is in accordance with the findings of recent studies, which have established that because Ni has a lower rate of water exchange than Fe (see above), Ni reacts more slowly with sulfides than Fe, and Ni therefore tends to be incorporated into pyrite rather than forming sulfides.

The DTMP of Cu was similar or even higher than the DOP (Figure 10), because the kinetics of the reaction between Cu and sulfides is faster than that between Fe and sulfides. This implies that in reduced sediments, Cu may react to form sulfides (see e.g. Zaggia and Zonta (1997)), which would also appear as part of the pyrite fraction as they are soluble in HNO_3 but not in 1 N HCl (Cooper and Morse 1998).

The plot of DTMP of Mn versus DOP showed that incorporation of Mn into the pyrite phase increased considerably from a degree of pyritization of Fe of around 50% (Figure 10), as found by other authors (Huerta-Díaz and Morse 1992; Morse and Luther 1999), and that there were strongly reducing conditions (Eh < -100 mV). Morse and Luther (1999) explained this by the fact that the reduction of Mn (IV) oxides occurs before sulfate reduction is initiated. Under suboxic conditions, the solubility of Mn appears to be controlled by carbonates, in particular rhodocrosite-calcite (Middelburg et al. 1987; Böttcher 1998), or by a dolomite type Ca-Mn carbonate (kutnahorite; Middelburg et al. (1987) and Mucci (1988)); thus, most of the Mn (II) can precipitate as carbonate before sulfate reduction occurs, and therefore there is no Mn left available to form manganese sulfides. Furthermore, the solubility of manganese sulfides (e.g. MnS, alabandite, pKsp = −1.3; Robie (1966)) is greater than that of iron sulfides (amorphous FeS: pKsp = −2.95; mackinawite: pKsp = −3.75; greigite: pKsp = −4.1; pyrite: pKsp = −15.4; Berner (1967)), thus large amounts of reactive Fe^{2+} impede the formation of MnS. The clear increase in pyritization of Mn (II) with degrees of pyritization of Fe (DOP-dithionite) higher than 50 % may indicate that the reactive-Fe starts to become limiting at this point (Morse and Luther 1999). This idea is supported by the results obtained when we consider the reactive-Fe to consist entirely of amorphous forms (Fe soluble in ascorbate, Figure 11). Pyritization of Mn occurred when the amorphous Fe was al-

most totally pyritized (DOP-ascorbate 85–95%), i.e. when Mn is more likely to co-precipirate with pyrite than to form MnS (see below).

The level of Zn incorporated into the pyrite phase was low (Figure 8), and only occurred under strongly reducing conditions (Eh < −100 mV). However, as with Cu, the water-exchange rate of Zn is faster than that of Fe and furthermore, because the solubility product of the different zinc sulfides is much lower than that of iron sulfides (e.g. ZnS: Kps: = −24.70; Stumm and Morgan (1981)), they will be formed and precipitated first. The Zn present in these types of soils can thus react to form sulfide minerals (e.g. sphalerite). In fact, zinc sulfide has been found in salt marsh sediments in previous studies using SEM-EDS and analyses of chemical extractions (Luther et al. 1980; Kitano et al. 1980; Lindau and Hosser 1982; Lee and Kittrick 1984; Zaggia and Zonta 1997). The main reason that low degrees of pyritization were measured is that zinc sulfides are soluble in 1N HCl and are thus included mainly in the reactive and not the pyrite fraction (Cooper and Morse 1998; Morse and Luther 1999). The Zn detected in the pyrite fraction in the most strongly reduced soils must therefore be a fraction of Zn coprecipitated with pyrite, which would explain the highly significant correlation between Zn and pyrite-Fe (Figure 9).

The pyrite fraction of the remaining trace metals was also strongly correlated with pyrite-Fe (Figure 9). This appears to indicate that under strongly reducing conditions, there is coprecipitation of Fe and trace metals, independently of the previous considerations. A significant increase in the DOP-dithionite was obtained at Eh values lower than −100 mV (Otero 2000). In this situation, the redox buffer produced by oxyhydroxides of Fe has been overcome, thus we can assume that there must be high concentrations of Fe (II) in the interstitial water. On the basis of the concentration of ascorbate-Fe plus pyrite-Fe measured in the solid phase, the concentration of Fe may be 40 to 1,000 times greater than that of the trace metals. Under these conditions (the presence of sulfides, slight acidity and Fe^{2+}), the most probable situation, from a kinetic point of view (see Howarth (1979)), is that pyrite will be formed and the other trace metals coprecipitated along with it. This is in accordance with previous observations and microanalyses carried out using SEM-EDS (scanning electron microscopy-energy dispersive X-ray spectrometry), which demonstrated the presence of trace metals (mainly Cu) associated with framboidal pyrite, but which never detected pure metal sulfide (Otero 2000). Similarly, Luther et al. (1980) found that MnS and NiS were always incorporated into pyrite or iron monosulfides, and Griffin et al. (1989) found highly significant correlations between pyrite-Fe and Ni extracted with hydrogen peroxide.

Conclusions

The redox conditions varied greatly among the salt-marsh soils under study. Results showed that the thermodynamic and kinetic properties of each metal appear to be more important in determining the concentration of trace metals in the pyrite

fraction than the concentration in the reactive fraction, or even the redox status of the soil. Thus, the high degree of pyritization of Cu found (higher than that of dithionite-Fe) was due to faster reaction kinetics between Cu and sulfides than between Fe and sulfides. Copper therefore occurs in sediments as sulfides or incorporated into pyrite. The DMTP values for Zn were expected to be similar to those for Cu, however they were very low, presumably because ZnS is soluble in 1N HCl. Nickel did not react by forming sulfides, but was progressively incorporated into pyrite as shown by the increase in DOP. The DTMP for Mn increased considerably when strongly reducing conditions prevailed in the soils and the amorphous forms of Fe were almost totally pyritized; it appears that under reducing conditions, the solubility of Mn is controlled by the presence of carbonates. Chromium did not form stable sulfides and did not tend to be incorporated into pyrite, it precipitated as a hydroxide in reduced soils or was found associated with organic matter.

Acknowledgements

This research was supported by the Spanish Government (AMB94.0293). X.L.O. was supported by an FPI grant from the Spanish Government. We thank Dr M.A. Huerta-Díaz for his valuable comments on the first draft of this manuscript and for providing the results of DTMP in different marine environments. We also thank Edgar Romero for his help in sampling soils. Finally, we are grateful for the comments of three anonymous referees, which helped to improve the original version of this manuscript.

References

Berner R.A. 1967. Thermodynamic stability and sedimentary iron sulfides. Am. J. Sci. 265: 773–785.

Berner R.A. 1970. Sedimentary pyrite formation. Am. J. Sci. 268: 1–23.

Boesen C. and Postma D. 1988. Pyrite formation in anoxic environments of the Baltic. Am. J. Sci. 288: 575–603.

Böttcher M.E. 1998. Manganese(II) partitioning during experimental precipitation of rhodochrosite-calcite solid solutions from aqueous solutions. Mar. Chem. 62: 287–297.

Bottrell S.H., Hayes P.J., Bannon M. and Williams G.M. 1995. Bacterial sulfate reduction and pyrite formation in a polluted sand aquifer. Geomicrobiology J. 13: 75–90.

Boulegue J., Lord C.J. III and Church T.M. 1982. Sulfur speciation and associated trace metals (Fe, Cu) in pore waters of Great Marsh, Delaware. Geochim Cosmochim. Acta 46: 453–464.

Bruland K.W., Franks R.P., Knauer G.A. and Martin J.H. 1979. Sampling and analytical methods for the nanogram per liter determination of copper, cadmium, zinc, and nickel in seawater. Anal. Chim. Acta 105: 233–241.

Burgess J. 1988. Ions in solution: Basic principles of chemical interactions. Hordwood-Ellis, Willey.

Canfield D.E. and Berner R.A. 1987. Dissolution and pyritization of magnetite in anoxic marine sediments. Geochim. Cosmochim Acta 51: 645–659.

Canfield D.E., Raiswell R. and Bottrell S. 1992. The reactivity of sedimentary minerals towards sulfide. Am. J. Sci. 292: 659–683.

Cline J.E. 1969. Spectrophotometric determination of hydrogen sulfide in natural waters. Limnol. Oceanogr. 14: 454–458.

Cooper D.C. and Morse J.W. 1998. Extractability of metal sulfide minerals in acidic solutions: Application to environmental studies of trace metal contamination. Environ. Sci. Technol. 32: 1076–1078.

Eary L.E. and Rai D. 1989. Kinetics of chromate reduction by ferrous ions. Amer. J. Sci. 289: 180–213.

Fendorf S.E. 1995. Surface reactions of chromium in soils and waters. Geoderma 67: 55–71.

Ferdelman T. 1988. The distribution of sulfur, iron, manganese, copper and uranium in a salt marsh sediment core as determined by a sequential extraction method. Masters thesis, Univ. Delaware.

Gardner L.R. 1990. Simulation of diagenesis of carbon, sulfur and dissolved oxygen in salt marsh sediments. Ecol. Monogr. 60: 91–111.

Gardner L.R., Wolaver T.G. and Mitchell M. 1988. Spatial variations in the sulfur chemistry of salt marsh sediments at North Inlet, South Carolina. J. Marine Research 46: 815–836.

Giblin A.E., Luther G.W. III and Valiela I. 1986. Trace metals in salt marsh sediments contaminated with sewage sludge. Estuarine. Coastal and Shelf Science 23: 477–498.

Griffin T.M., Rabenhorts M.C. and Fanning D.S. 1989. Iron and trace metals in some tidal marsh soils of the Chesapeake Bay. Soil Sci. Soc. Am. J. 53: 1010–1019.

Guo T., DeLaunem R.D. and Patrick W.H. jr 1997. The influence of sediment redox chemistry on chemically active forms of arsenic, cadmium, chromium, and zinc in estuarine sediment. Environment International 23: 305–316.

Howarth R.W. 1979. Pyrite: Its rapid formation in a salt marsh and its importance in ecosystem metabolism. Science 203: 49–51.

Howarth R.W. 1984. The ecological significance of sulfur in the energy of salt marsh and coastal marine sediments. Biogeochem. 1: 5–27.

Howarth R.W. and Merkel S. 1984. Pyrite formation and measurement of reduction in salt marsh sediments. Linmol. Oceanogr. 29: 598–608.

Howarth R.W. and Teal J.M. 1979. Sulfate reduction in a New England salt marsh. Limnol. Oceanogr. 24: 999–1013.

Howes B.L., Howarth R.W., Teal J.M. and Valiela I. 1981. Oxidation -reduction potentials in a salt marsh: Spacial patterns and interactions with primary production. Limnol. Oceanogr. 26: 350–360.

Huerta-Díaz M.A. 1989. Geochemistry of trace metals associated with sedimentary pyrite from anoxic marine environments. PhD Dissertation, Texas A&M University.

Huerta-Díaz M.A. and Morse J.W. 1990. A quantitative method for determination of trace metal concentrations in sedimentary pyrite. Mar. Chem. 29: 119–144.

Huerta-Díaz M.A. and Morse J.W. 1992. Pyritization of trace metals in anoxic marine sediments. Geochim. Cosmochim. Acta 56: 2681–2702.

Huerta-Díaz M.A., Tessier A. and Carignan R. 1998. Geochemistry of trace metals associated with reduced sulfur in freshwater sediments. Appl. Geochem. 13: 113–233.

Instituto Hidrográfico de la Marina 1993. Anuario de Mareas. Servicio de Publicaciones de la Armada, Cádiz, Spain.

Jenne E.A. 1968. Controls on Mn, Fe, Cu, Ni, Zn concentrations in soils and waters: significant role of hydrous Mn and Fe oxides. Adv. Chem. Ser. 73: 337–387.

Jordan T.E. 1985. Nutrient chemistry and hydrology of interstitial water in brackish tidal marshes of Chesapeake Bay. Estuarine Coastal Shelf Sci. 21: 45–55.

Khawary A.M., Henrion G. and Henrion R. 1992. Sorption kinetics of Cu and Zn ions on Mn (IV) and Fe (III) oxides. Fressenius Envir. Bull (supplementum) S7–S12: 7–12.

Kitano Y., Sakata M. and Matsumoto E. 1980. Partitioning of heavy metals into minerals and organic fractions in a sediment core from Tokyo Bay. Geochim. Cosmochim. Acta 44: 1279–1285.

Kostka J.E. and Luther G.W. III 1994. Partitioning and speciation of soil phase iron in saltmarsh sediments. Geochim. Cosmochim. Acta 58: 1701–1710.

Kostka J.E. and Luther G.W. III 1995. Seasonal cycling of Fe in saltmarsh sediments. Biogeochem. 29: 159–181.

Lee F.Y. and Kittrick J.A. 1984. Electron microprobe analysis of elements associated with zinc and copper in an oxidizing and an anaerobic soil environment. Soil Sci. Soc. Am. J. 48: 548–554.

Lindau C.W. and Hosser L.R. 1982. Sediment fractionation of Cu, Ni, Zn, Cr, Mn, and Fe in one experimental and three natural marshes. J. Environ. Qual. 11: 540–545.

Lord C.L. III and Church T.M. 1983. The geochemistry of salt marshes: sedimentary ion diffusion sulfate reduction and pyritization. Geochim Cosmochim Acta 47: 1381–1391.

Lu C. and Chen K. 1977. Migration of trace metals in interfaces of seawater and polluted surficial sediments. Environ. Sci. Technol. 11: 174–182.

Luther G.W. III, Ferdelman T.G., Kostka J.E., Tsamakis E.J. and Church T.M. 1991. Temporal and spatial variability of reduced sulfur species (FeS_2, S_2O_2) and pore water parameters in salt marsh sediments. Biogeochem. 14: 57–88.

Luther G.W. III, Meyerson A.L., Krajewski J.J. and Hires R. 1980. Metal sulfide in estuarine sediments. J. Sediment. Petrol. 50: 1117–1120.

Middelburg J.J., de Lange G.J. and van der Weijden C.H. 1987. Manganese solubility control in marine pore waters. Geochim. Cosmochim. Acta 51: 759–763.

Morse J.W. 1994. Interactions of trace metals with authigenic sulfide minerals: Implications for their bioavailability. Mar. Chem. 46: 1–6.

Morse J.W. and Luther G.W. III 1999. Chemical influences on trace metal-sulfide interactions in anoxic sediments. Geochim. Cosmochim. Acta 63: 3373–3378.

Mucci A. 1988. Manganese uptake during calcite precipitation from seawater: Conditions leading to the formation of a pseudokutnahorite. Geochim. Cosmochim Acta 52: 1859–1868.

Munsell Color Company 1975. Munsell Soil Color Charts. Munsell Color Co. (ed)., Baltimore, MD, USA.

Otero X.L. 2000. Biogeoquímica de metales pesados en ambientes sedimentarios marinos. I.- Fluvisoles de las marismas de la Ría de Ortigueira (NW Península Ibérica). II.-Fosa Hidrotermal de Guaymas (Golfo de California-México). PhD Dissertation, Universidad de Santiago de Compostela, Spain.

Otero X.L., Huerta-Díaz M.A. and Macías F. 2000a. Heavy metal geochemistry of saltmarsh soils from the ría of Ortigueira (Mafic and ultramafic area, NW Iberian Peninsula). Environm. Pollut. 110: 285–296.

Otero X.L., Sánchez J.M. and Macías F. 2000b. Bioaccumulation of heavy metals in thionic fluvisols by a marine polychaete (*Nereis diversicolor*): The role of metal sulfide. J. Environ. Qual 29: 1133–1141.

Postma D. and Jakobsen R. 1996. Redox zonation: Equilibrium constraints on the Fe (III)/SO_4 reduction interface. Geochim. Cosmochim. Acta 60: 3169–3175.

Price J., Ewing K., Woo M.K. and Kersaw K.A. 1988. Vegetation patterns in James Bay Coastal marshes. II. Effects of hydrology on salinity and vegetation. Can. J. Bot. 66: 2586–2594.

Rai D., Eary L.E. and Zachara J.M. 1989. Environmental chemistry of chromium. Sci. Total Environ. 86: 15–23.

Raiswell R., Canfield D.E. and Berner R.A. 1994. A comparasion of iron extraction methods of degree of pyritisation and the recognition of iron-limited formation. Chemical Geology 111: 101–110.

Robie R.A. 1966. Thermodynamic properties of minerals. Mem. Am. Geol. Soc. 97: 437–458.

Russell P.J., Flowers T.J. and Hutchings M.J. 1985. Comparison of niche breadths and overlaps of halophytes on salt marshes of differing diversity. Vegetatio 61: 171–178.

Sager M. 1992. Chemical speciation and environmental mobility of heavy metals in sediments and soils. In: Stoeppler (ed.), Hazardous metals in the environment. Elsevier Science Publisher, pp. 133–175.

Sánchez J.M. 1995. Caracterización florística y fitosociológica de las Rías de Ortigueira y Ladrido (Noroeste de la Península Ibérica) en relación con factores ambientales. PhD Dissertation, Facultad de Farmacia. Universidad de Santiago de Compostela, Spain.

Sánchez J.M., Izco J. and Medrano M. 1996. Relationships between vegetation zonation and altitude in a salt-marsh system in northwest Spain. J. Vegetation Science 7: 696–702.

Sánchez J.M., Otero X.L. and Izco J. 1998. Relationships between vegetation and environmental characteristics in a salt-marsh system on the coast of Northwest Spain. Plant Ecology 136: 1–8.

Saunders J.A., Pritchett M.A. and Cook R.B. 1997. Geochemistry of biogenic pyrite and ferromanganese coating from a small watershed: A bacterial connection? Geomicrobiol. J. 14: 203–217.

Sass B.M. and Rai D. 1987. Solubility of amorphous chromium(III)-iron(III) hydroxides solid solutions. Inorg. Chem. 26: 2228–2232.

Schoer J. 1985. Iron-oxy-hydroxides and their significance to the behavior of heavy metals in estuaries. Environ. Technol. Lett. 6: 189–202.

Smillie R.H., Hunter K. and Loutit M. 1981. Reduction of chromium (VI) by bacterially produced hydrogen sulphide in a marine environment. Water Res. 15: 1351–1354.

Stumm W. and Morgan J.J. 1981. Aquatic Chemistry. John Wiley & Sons, New York.

Systat INC 1992. SYSTAT for Windows Version. 5th edn. Systat INC, Evanston, IL, USA.

Valiela I., Teal J.M. and Persson N.Y. 1976. Production and dynamics of experimentally enriched salt marsh vegetation: Bellowground biomass. Limnol. Oceanogr. 21: 245–252.

Van Calsteren P.W.C. 1978. Geochemistry of the polymetamorphic mafic-ultramafic complex at Cabo Ortegal (NW Spain). Lithos 11: 61–72.

Van Cappellen P. and Wang Y. 1996. Cycling of iron and manganese in surface sediments: a general theory for the coupled transport and reduction of carbon, oxygen, nitrogen, sulfur, iron and manganese. Am. J. Sci. 296: 197–243.

Wiegert R.G., Pomeroy L.R. and Wiebe W.J. 1981. Ecology of salt marsh: An Introduction. In: Pomeroy and Wiegert (eds), The Ecology of a Salt Marsh. Springer-Verlag, New York, pp. 3–18.

Wilkin R.T. and Barnes H.L. 1997. Pyrite formation in an anoxic estuarine basin. Am. J. Sci. 297: 620–650.

Zaggia L. and Zonta R. 1997. Metal-sulphide formation in the contaminated anoxic sludge of the Venice canals. Appl. Geochem. 12: 527–536.